A new hyperspectral index of biological crust in remote sensing

Xu Ma[1*], *Qun* Luo[1], *Hui* Sun[1], and *Ke* Du[1]

[1] College of Geography and Remote sensing Sciences, Xinjiang key Laboratory of Oasis Ecology, Urumqi 830064, China;

Abstract. Biological crusts (BC) are an organic complex, composed of bacteria, cyanobacteria, diatoms, green algae, tiny fungi, ground jackets, and moss plants, as well as other related organisms. BC is distributed about 40% in arid areas, which is one of the important surface landscapes in the intertwined area between oasis and desert. The relationship between BC and drought is close, which can be used to monitor desertification and water resources in remote sensing. However, the current monitoring of BC uses a simple BC index composed of multi-spectrum to extract its area distribution in remote sensing, which makes it difficult to accurately detect its area. This study considers the characteristic bands in the hyper-spectrum cure and designs a hyperspectral index of BS, i.e., HBCI. The HBCI is used, and we successfully estimated the area of biological soil crusts (Kappa=0.86) in the PRISMA image. This finding has help for the regional climate change research.

1 Introduction

The biological crusts (BC) have been distributed in most desert areas in the world, the coverage in some semi-fixed deserts can even account for 70% [1]. With the influence of climate change and human activities, the fractional biocrust coverage in the desert areas has been severely damaged. The decrease in the fractional biocrust coverage has led to the erosion of the desert, then this phenomenon increases in the movement of the dunes [2]. Therefore, how to identify BC has attracted much attention. There are many methods to estimate the area of biological crusts, including direct spectral analysis method, index method with algebraic operation, and index method based on radiative transfer theory [3]. In the direct spectral analysis method, the characteristic bands that can distinguish between biocrusts and the 'background' (e.g., sand or soil) are selected to analyse the spectrum of biocrusts, e.g., Wessels and van Vuuren used characteristic bands (green band, red band, and near-infrared band) to compose false color images to estimate the area covered by lichen-dominated crusts [4].

*Corresponding author: e-mail: maxu2020@xju.edu.cn

Similarly, 1730nm and 2100nm are used by Ager and Milton to estimate the area covered by lichen-covered rock surfaces in remotely sensed images [5]. To area of BC in the remote sensing, Karnieli and Sarafis used the blue band to identify phycobilin in the cyanobacteria-dominated crusts [6]. In early studies, the direct spectral analysis method only concentrates on the estimation of a single species of biocrust [7]. To estimate biocrusts with multispecies, O'Neill (1994) used the 2080nm and 2100nm to estimate the biocrusts areas [8]. However, biocrusts are organic complexes with mixed spectra, which can cause uncertainty in the detection results. Therefore, the index method is widely used to estimate the area of biological soil crusts [9].

Compared with the index method based on radiative transfer theory, the mathematical physical mechanism of the index method with algebraic operation is relatively easy to promote. Therefore, index method with algebraic operation is widely used [10]. To estimate the area of cyanobacterial crusts, a crust index (CI) was developed to extract the area covered by cyanobacterial crusts in desert areas [11]. However, biocrusts not only include cyanobacterial crusts but also include lichen-dominated crusts and moss-dominated crusts in desert areas [12]. Therefore, a biological soil crust index (BSCI) was developed, and BSCI was successfully estimated area of BC in the Gurbantunggut Desert of China [13]. These indexes are designed based on multi-spectral images [14]. With the development of hyperspectral remote sensing, more and more the hyperspectral image is used to identify the land cover in remote sensing [15]. Compared with the previous multi-spectral image, the hyperspectral image has a significant advantage [16]. The BC is difficult to distinguish between multi-spectral remote sensing images, hyperspectral image can obtain a more detailed spectral band, which can be used to analysis the characteristics of the spectral curve of BC [17].

We try to analyze the characteristic bands of BC and design a hyperspectral index of BC. In this study, we measured the spectral curve of BC, and then the first derivative and second derivative were used to determine the characteristic band of BC. The algebraic operation is used, and a new hyperspectral index of BC was designed, i.e., HBCI.

2 Materials and methods

It is largest fixed semi-fixed desert in China, its area is an area of about $4.88 \times 10^4 km^2$. In this study, we selected the southern edge of the Gurbantunggut Desert in Xinjiang, which is in the Hui Autonomous Prefecture of Changji, see **Fig. 1(a)**.

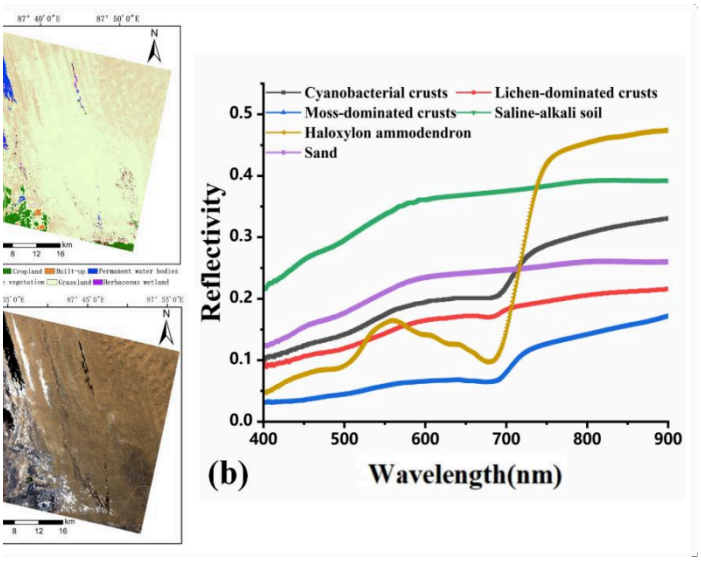

Fig. 1. Map, spectral curve and PRISMA image. (a) Land cover in the Changji of Gurbantunggut Desert; (b) and spectral curve of BC, soil, and desert vegetation in the Gurbantunggut Desert; (c) hyperspectral image of PRISMA.

To measure the spectral curve of BC, we have chosen 49 quadrats to collect samples of BC, including blue-green algae, lichens, and bryophytes. The samples of BC were brought back to the laboratory and then used an ASD spectrometer (Field Spec3) to measure these spectrums. To validate the accuracy calculated by the new hyperspectral index of BS, 49 quadrats were used as a reference to validate. In addition, to distinguish the differences among BC, soil, and desert vegetation, the spectrum of soil and the spectrum of desert vegetation are also measured. The spectral curve is shown in Fig. 1(b). For the hyperspectral image, we used the PRISMA image (Hyperspectral, 2D products) obtained from April 6, 2022. It includes 237 bands from 400~2500 nm, and the space resolution is 30 m (Fig. 1(c)). To obtain the surface reflectance, atmospheric correction was addressed using ENVI software.

To determine the characteristic bands, the first derivative and second derivative are used, i.e.,

$$f'(x_0) = \lim_{\Delta \to 0} \frac{\Delta y}{\Delta x} = \lim_{\Delta \to 0} \frac{f(x_0 + \Delta x) - f(x_0)}{\Delta x} \quad (1)$$

$$f'' = \frac{d^2 f[x]}{dx^2} \quad (2)$$

Where x represents the reflectance at a certain band. Through the first derivative and second derivative, we found that 406 nm, 423nm, 527nm, and 934nm are the characteristic bands (**Fig. 2**).

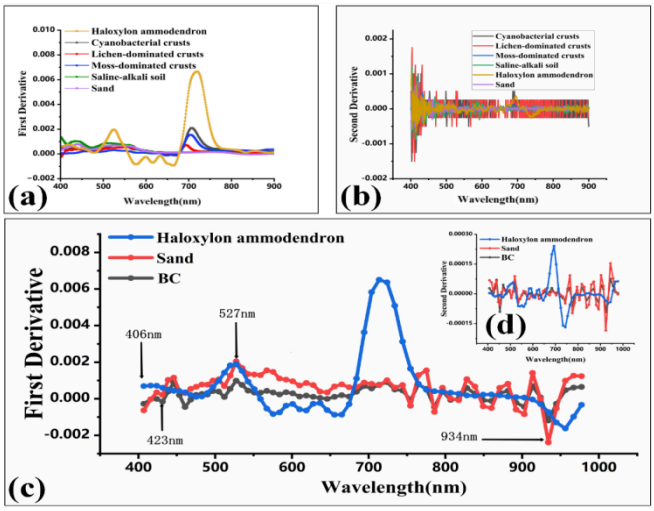

Fig.2. First derivative and second derivative for biological crusts, sand, and desert vegetation. (a) first derivative calculated from measure data, (b) first derivative calculated from PRISMA image, (a) second derivative calculated from measure data,(b) second derivative calculated from PRISMA image.

After the algebraic operation, we designed a new hyperspectral index of BC, i.e.,

$$HBCI = -\frac{R_{B17} - \left(R_{B1} + R_{B3}\right)}{R_{B17} + R_{B59}} \tag{3}$$

Where R_{B1} is 406 nm, R_{B3} is 423nm, R_{B17} is 527nm, and R_{B59} is 934nm. **Fig. 3** show shows the distinction capabilities of each band.

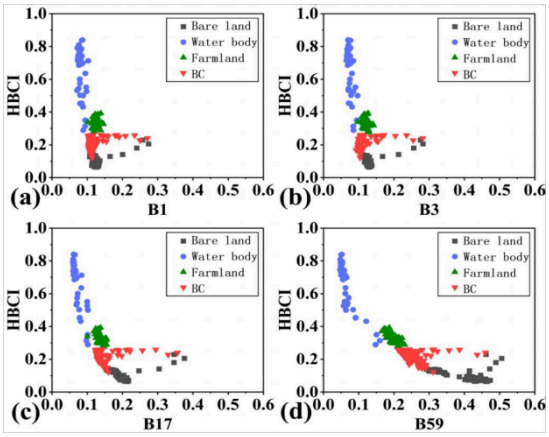

Fig. 3. The relationship between HBCI in each band.

3 Results and discussion

Fig. 4(a) shows results calculated by HBCI. the BC is mainly distributed in the southeast of the study area (black area). The main reason is that the area is close to the oasis. In the northern and northeast of the study area, the distribution of BC is relatively scattered, it can be found that BC and dunes are staggered distribution (yellow and black area). Compared with the FBC, the area of BC calculated by HBCI and measurement data have a high correlation (R2=0.8413 in Fig. 4(b)). From the validated results of area, HBCI is used to distinguish BC and the calculation accuracy of 0.86, when 100 validated points are used.

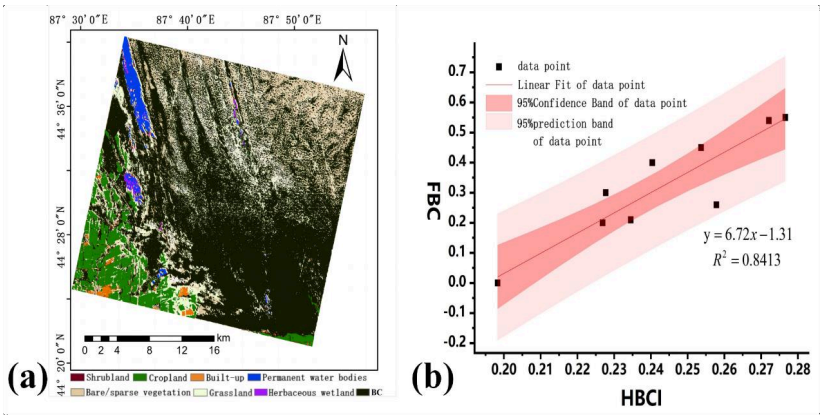

Fig. 4. The results of BC calculated by HBCI. (a) Distribution map of BC, (b) comparison results between measuring data and by HBCI. FBC= fractional biocrust coverage.

Table 1. Table of the confusion matrix for HBCI classification

	Other	Biological crusts
Other	90	10
Biological crusts	4	96
	Kappa=0.86	Accuracy=93%

Acknowledgments

This work was supported by the Open Project of the Key Laboratory in the Xinjiang Uyghur Autonomous Region (grant number: 2022D04051), the National Natural Science Foundation of China (grant number: 42201390), the Cooperative research project of "Chunhui Program" of Chinese Ministry of Education (grant number: HZKY20220609), the university of basic scientific business fees for scientific research projects in the Xinjiang Uygur Autonomous Region (grant number: XJEDU2022P014), PhD starts funds of Xinjiang University (grant number: 620321021), the Postdoctoral Research Foundation of China (grant number: 2021M702748), Tian chi Doctoral

Program in the Xinjiang Uygur Autonomous Region (grant number: TCBS202127), the Open Fund for State Key Laboratory (grant number: G2023-02-05), Xinjiang University Research Institute of Central Asia Project (grant number: 24ZYYB003).

Authors' contribution

The following statements may be used "Conceptualization, X.M.; Methodology, X.M. K.D.; Software, K.D.; Formal Analysis, K.D.; Investigation, X.M. and H. S.; Resources, X.M.; Writing – Original Draft Preparation, X.M.; Writing – Review & Editing, X.M.; Visualization, H. S. and Q. L.; Supervision, X.M.; Project Administration, X.M.; Funding Acquisition, X.M."

4 Conclusion

In this study, we used the first derivative and second derivatives to extract the spectral characteristic bands of typical elements in arid areas, which are 406nm, 423nm, 527nm and 934nm. These characteristic bands correspond to B1, B3, B17 and B59 bands of PRISMA image data. Based on this, we designed a new hyperspectral BC index, i.e., HBCI. To validate the relationship between HBCI and a single band, we constructed a feature space diagram between the characteristic band and HBCI. From the results, the four single bands can distinguish BC, bare land, water body and farmland well, among which the classification effect of B59 band is better, and the other three bands are also very important, indicating that the band selection is effective. In summary, the HBCI proposed by us has a high accuracy in calculating the area of BC, among which the overall accuracy of BC classification reaches 93%, and the Kappa coefficient reaches 0.86, indicating that the hyperspectral BC index proposed by us can be well applied to the extraction of BC in desert or arid areas. In addition, HBCI was highly correlated with FBC (R2=0.8413), which has a potential area estimate of FBC. Our index represents a new kind of hyperspectral index and has great application potential in the field of hyperspectral remote sensing.

Reference

1. Chen, J., Yuan Zhang, M., Wang, L., Shimazaki, H., & Tamura, M. A new index for mapping lichen-dominated biological soil crusts in desert areas. Remote Sensing of Environment, **96(2)**, 165–175. (2005). https://doi.org/10.1016/j.rse.2005.02.011
2. Belnap, J., Büdel, B., & Lange, O. L. Biological Soil Crusts: Characteristics and Distribution. In J. Belnap & O. L. Lange (Eds.), Biological Soil Crusts: Structure, Function, and Management (pp. 3–30). Springer. (2003).https://doi.org/10.1007/978-3-642-56475-8_1
3. Sun, H., Ma, X., Liu, Y., Zhou, G., Ding, J., Lu, L., Wang, T., Yang, Q., Shu, Q., & Zhang, F. A New Multiangle Method for Estimating Fractional Biocrust Coverage From Sentinel-2 Data in Arid Areas. IEEE Transactions on Geoscience and Remote Sensing, **62**, 1–15. (2024).https://doi.org/10.1109/TGRS.2024.3361249
4. Wessels, D. C. J. & V. V. D. R. J. (1986). Landsat imagery—Its possible use in mapping the distribution of major Lichen Communities in the Namib Desert, South West Africa. Madoqua, **(4)**, 369–373. 1986 https://doi.org/10.10520/AJA10115498_474

5. Ager, C. M., & Milton, N. M. Spectral reflectance of lichens and their effects on the reflectance of rock substrates. GEOPHYSICS, **52(7)**, 898–906. (1987). https://doi.org/10.1190/1.1442360
6. Karnieli, A., & Sarafis, V. . Reflectance spectrophotometry of cyanobacteria within soil crusts—A diagnostic tool. International Journal of Remote Sensing, **17(8)**, 1609–1615.(1996) https://doi.org/10.1080/01431169608948726
7. 7.Weber, B., Olehowski, C., Knerr, T., Hill, J., Deutschewitz, K., Wessels, D. C. J., Eitel, B., & Büdel, B. A new approach for mapping of Biological Soil Crusts in semidesert areas with hyperspectral imagery. Remote Sensing of Environment, **112(5)**, 2187–2201.(2008).https://doi.org/10.1016/j.rse.2007.09.014
8. O'NEILL, A. L. Reflectance spectra of microphytic soil crusts in semi-arid Australia. International Journal of Remote Sensing, **15(3)**, 675–681. (1994). https://doi.org/10.1080/01431169408954106
9. Wang, Z., Wu, B., Zhang, M., Zeng, H., Yang, L., Tian, F., Ma, Z., & Wu, H. Indices enhance biological soil crust mapping in sandy and desert lands. Remote Sensing of Environment, 278, 113078. (2022). https://doi.org/10.1016/j.rse.2022.113078
10. Martinson, W. S., & Barton, P. I. A Differentiation Index for Partial Differential-Algebraic Equations. SIAM Journal on Scientific Computing, **21(6)**, 2295–2315.(2000). https://doi.org/10.1137/S1064827598332229
11. Román, J. R., Rodríguez-Caballero, E., Rodríguez-Lozano, B., Roncero-Ramos, B., Chamizo, S., Águila-Carricondo, P., & Cantón, Y. Spectral Response Analysis: An Indirect and Non-Destructive Methodology for the Chlorophyll Quantification of Biocrusts. Remote Sensing, **11(11),** Article 11. (2019). https://doi.org/10.3390/rs11111350
12. Sosa-Quintero, J., Godínez-Alvarez, H., Camargo-Ricalde, S. L., Gutiérrez-Gutiérrez, M., Huber-Sannwald, E., Jiménez-Aguilar, A., Maya-Delgado, Y., Mendoza-Aguilar, D., Montaño, N. M., Pando-Moreno, M., & Rivera-Aguilar, V. Biocrusts in Mexican deserts and semideserts: A review of their species composition, ecology, and ecosystem function. Journal of Arid Environments, 199, 104712. (2022). https://doi.org/10.1016/j.jaridenv.2022.104712
13. .Zhang, Y. M., Chen, J., Wang, L., Wang, X. Q., & Gu, Z. H. The spatial distribution patterns of biological soil crusts in the Gurbantunggut Desert, Northern Xinjiang, China. Journal of Arid Environments, **68(4)**, 599–610. (2007). https://doi.org/10.1016/j.jaridenv.2006.06.012
14. .Crucil, G., & Van Oost, K. (2021). Towards Mapping of Soil Crust Using Multispectral Imaging. Sensors, **21(5)**, Article 5. https://doi.org/10.3390/s21051850
15. 15.Navin, M. S., & Agilandeeswari, L. Multispectral and hyperspectral images based land use / land cover change prediction analysis: An extensive review. Multimedia Tools and Applications, **79(39),** 29751–29774. (2020). https://doi.org/10.1007/s11042-020-09531-z
16. Vali, A., Comai, S., & Matteucci, M. Deep Learning for Land Use and Land Cover Classification Based on Hyperspectral and Multispectral Earth Observation Data: A Review. Remote Sensing, **12(15)**, Article 15.(2020). https://doi.org/10.3390/rs12152495
17. Lehnert, L. W., Jung, P., Obermeier, W. A., Büdel, B., & Bendix, J.Estimating Net Photosynthesis of Biological Soil Crusts in the Atacama Using Hyperspectral Remote Sensing. Remote Sensing, **10(6)**, Article 6. (2018). https://doi.org/10.3390/rs10060891